Advances in Theoretical and Applied Mathematics
ISSN 0973-4554 Volume 12, Number 1 (2017), pp. 15-38

http://www.ripublication.com

MHD Pulsatile Slip Flow of Blood through Porous Medium in an Inclined Stenosed Tapered Artery in Presence of Body Acceleration

Lukendra Kakati[1], Dhruba Prasad Barua[2], Nazibuddin Ahmed[3], Karabi Dutta Choudhury[4]

[1]*Department of Mathematics, Lanka Mahavidyalaya, Lanka, Nagaon-782446, Assam, India.*

[2] *Puberun path, House number-13, Hatigaon main road, Guwahati-781038, Assam, India*

[3]*Department of Mathematics, Gauhati University, Guwahati-781014. Assam, India*

[4] *Department of Mathematics, Assam University, Silchar- 788011, Assam, India.*

Abstract

In the present Paper, the Authors have investigated the pulsatile flow of blood through a porous medium with *constant permeability*, in an inclined tapered artery with mild stenosis. The flow of blood is considered to be Newtonian. The presence of an azimuthal uniform magnetic field is assumed. The flow takes place under body acceleration and a slip velocity is imposed at the stenosed arterial wall. By using Perturbation technique, the solutions for the flow field, wall shear stress, volumetric flux and the effective viscosity are obtained and their behaviors under the influence of various relevant parameters concerning the magnetic field, velocity slip, permeability, inclination etc. have been demonstrated pictorially and discussed. It is seen that the applied magnetic field, velocity slip, inclination and the permeability of the porous medium have significant influence on the flow field, wall shear stress, volumetric flow rate and the effective viscosity. For instance, the volumetric flow rate and the effective viscosity fall with a growth in the tapering angle. Further, the imposition of the slip velocity leads to a growth in each of axial velocity of blood and the volumetric flow rate. Furthermore, the

imposition of the magnetic field causes a decrease in each of axial velocity of blood, and the volumetric flow rate. However the effective viscosity increases with the increase in magnetic field strength.

Keywords: MHD, Pulsatile, Porous, Slip velocity, Blood flow, Stenosis, Inclined, Tapered

Mathematics Subject Classification: 76Z05, 74G10, 76W05

1. INTRODUCTION

The studies related to blood flow through stenosed arteries have garnered wide interest in the field of Bio-Medical research. Stenosis or atherosclerosis may be defined as the formation of some constriction in the inner arterial wall owing to the deposition of lipoproteins and fatty acids (atherosclerotic plaques) in the lumen of the artery. Such constrictions lead to considerable change in the flow of blood, the pressure distribution and the wall shear stress, thereby impeding the normal circulatory processes and consequently leading to cardiovascular diseases. Even for mild atherosclerosis, the velocity gradient in the stenosed wall is steep owing to the increased core velocity. This results in comparatively large shear stress on the arterial wall. Mathematical models of blood flow through arteries under diverse physiological situations were presented by several authors like Fung [1], McDonald [2], Zamir [3] and David et al. [4]. Theoretical and experimental investigations concerning flow of blood through stenosed arteries were presented by Young [5], Liu et al. [6], Yao and Li [7] and Mekheimer and El-Kot [8]. The human body may be subjected to body accelerations (vibrations) under certain situations such as riding a heavy vehicle or flying in a helicopter. This may cause health problems like vascular disorders and increased pulse rate. Studies related to blood flow under the influence of body acceleration were carried out by several research workers such as Sud and Sekhon [9] and El-Shahed [10]. The Pulsatile nature of blood flow in arteries may be attributed to the heart pulse pressure gradient. Studies in pulsatile blood flow were carried out by researchers like [10] and Elshehawey et al. [11]. The possibility of velocity slip at the blood vessel wall was investigated theoretically by Brunn [12] and Jones [13] and experimentally by Bennet [14] and Bugliarello and Hayden [15]. The methods to detect and determine slip experimentally at the blood vessel wall have been indicated by Astarita et al. [16] and Cheng [17] respectively. It was first Kolin [18] and later Korchevskii and Marochnik [19] who suggested the scope of electromagnetic fields in Bio-Medical studies. Barnothy [20] indicated that for biological systems, the heart rate decreases under the influence of an external magnetic field. In certain pathological circumstances, the distribution of fatty cholesterol and artery-clogging blood clots in the lumen of the coronary artery may be regarded as equivalent to a fictitious porous medium. Xu et al. [21] assumed the blood clot as a porous medium to investigate the transport characteristics of blood flow in the extension of multi-scale model by incorporating a detailed sub model of surface-mediated control of blood coagulation (Xu et al. [22, 23]). In general, blood is a non-Newtonian fluid.

However, it has been established that human blood exhibits Newtonian behavior at all rates of shear for hematocrits up to about 12% [24]. Further, in case of relatively larger blood vessels it is sensible to assume that blood has a constant viscosity, since the diameters of such vessels are large compared with the individual cell diameters and because shear rates are quite high for viscosity to be independent of them. Consequently, for such vessels the non-Newtonian character becomes unimportant and blood may be regarded as a Newtonian fluid.

In view of the aforementioned facts, we may cite the works done by Elshehawey et al. [11], Nagarani and Sarojamma [25], Shehawey and EL Sebaei [26], Tzirtzilakis [27], etc.

The aim of the present study is to investigate theoretically the nature of a pulsatile blood flow through a mildly stenosed, tapered artery under the combined influence of an azimuthal uniform magnetic field, slip velocity, body acceleration and permeability, when the artery is inclined to the vertical. The investigation is carried out by treating blood flow as Newtonian.

2. THE FORMULATION OF THE PROBLEM

For the present problem, we consider an axially symmetric, laminar, one-dimensional and fully developed flow of blood, through an inclined, tapered and constricted circular artery, in the presence of a time-dependent pressure gradient, body acceleration and a uniform circular (azimuthal) magnetic field of moderate intensity. Thus, the induced magnetic field is negligible. We assume that this constricted tapered artery has a rigid wall and that the artery is filled with a porous medium of constant permeability. Further, this tapered artery is inclined to the vertical and a slip velocity is imposed at the stenosed region of the arterial wall. Here, blood is assumed as a Newtonian fluid and the corresponding flow is considered to be Newtonian. The flow configuration is presented pictorially, in the section for figures.

The geometry of an arterial stenosis is (Liu et. al [29]), as below:

$$\bar{R}\left(\bar{z}\right)=\begin{cases}\bar{L}-m\left(\bar{z}+\bar{d}\right)-\dfrac{\bar{d}_s\cos\phi}{2}\left(1+\cos\dfrac{\pi\bar{z}}{\bar{d}_0}\right), & \text{for } \left|\bar{z}\right|\le\bar{d}_0\\ \bar{L}-m\left(\bar{z}+\bar{d}\right), & \text{for } \left|\bar{z}\right|>\bar{d}_0\end{cases} \tag{1}$$

Where $\bar{R}\left(\bar{z}\right)$ is the radius of the artery in the stenosed region, $\bar{L}$ is the constant arterial radius in the non-stenosed region, $\bar{d}_0$ is the half-length of the stenosis and $\bar{d}_s$ is the greatest height of the stenosis such that $\dfrac{\bar{d}_s}{\bar{L}}$ is less than unity for a mild stenosis. Here the radial velocity is very small due to the low Reynolds number flow through the artery with mild stenosis (Nagarani and Sarojamma [25]); hence we do not consider the radial velocity. Also, $m=\tan\phi$ represents the slope of the tapered

artery, where ϕ is the angle of tapering. Further, $\bar{d}_s \cos\phi$ is the height of the stenosis at a length $\bar{d}$ for the tapered artery.

In cylindrical coordinate system $\left(\bar{r},\bar{\theta},\bar{z}\right)$, the momentum equation governing the flow is deduced from Navier-Stokes equations of motion and presented as under:

$$\frac{\partial \bar{u}}{\partial \bar{t}} = \frac{1}{\rho}\bar{F}\left(\bar{t}\right) + g\cos\beta - \frac{1}{\rho}\frac{\partial \bar{P}}{\partial \bar{z}} + \upsilon\left(\frac{\partial^2 \bar{u}}{\partial \bar{r}^2} + \frac{1}{\bar{r}}\frac{\partial \bar{u}}{\partial \bar{r}}\right) - \frac{\sigma \bar{u}\bar{B}^2}{\rho} - \frac{\upsilon \bar{u}}{\bar{K}} \tag{2}$$

$$\frac{\partial \bar{P}}{\partial \bar{r}} = -g\rho Sin\beta \tag{3}$$

Where $\bar{u}$ denotes the velocity along the $\bar{z}$ - axis, $\bar{P}$ the pressure, ρ the density, $\bar{t}$ the time, $\bar{F}\left(\bar{t}\right)$ the body acceleration, $\bar{B}$ the applied magnetic field in azimuthal ($\bar{\theta}$) direction, υ the kinematic viscosity, σ the electrical conductivity, g the acceleration due to gravity, β the angle of inclination of the artery with the vertical and $\bar{K}$ the permeability of the porous medium.

The relevant boundary conditions are as under:

$$\bar{u} = \bar{V}_s \text{ at } \bar{r} = \bar{R}\left(\bar{z}\right) \tag{4}$$

$$\frac{\partial \bar{u}}{\partial \bar{r}} = 0 \text{ at } \bar{r} = 0 \tag{5}$$

Where $\bar{V}_s$ is the slip velocity at the stenosed region of the arterial wall. Clearly $\bar{u}$ must be finite on the axis of the tubular artery i.e. at $\bar{r} = 0$.

When $\bar{t} > 0$, periodic body acceleration $\bar{F}\left(\bar{t}\right)$ is imposed on the flow and this may be presented as under (Nagarani and Sarojamma [25]):

$$\bar{F}\left(\bar{t}\right) = f_0 \cos\left(\bar{\omega}_0 \bar{t} + \theta\right), \tag{6}$$

Where $\bar{\omega}_0 = 2\pi\bar{F}_b$, f_0 and $\bar{F}_b$ being respectively the amplitude of body acceleration and frequency (in Hertz) of body acceleration. Also, θ is the lead angle with respect to the heart action. $\bar{F}_b$ is taken to be so small that wave effect may be omitted (Nagarani and Sarojamma [25]).

Further, for $\bar{t} \geq 0$, the pressure gradient is assumed as:

$$-\frac{\partial \bar{P}\left(\bar{z},\bar{t}\right)}{\partial \bar{z}} = P_0\left(\bar{z}\right) + P_1\left(\bar{z}\right)\cos\left(\bar{\omega}_P \bar{t}\right) \tag{7}$$

Where $P_0\left(\bar{z}\right)$, $P_1\left(\bar{z}\right)$ are respectively the steady state pressure gradient and the amplitude of the oscillatory part of the pressure gradient. Further, $\bar{\omega}_P = 2\pi \bar{f}_P$ where $\bar{f}_P$ is the pulse rate frequency.

We make the following non-dimensional substitutions:

$$z = \frac{\bar{z}}{\bar{L}}, R\left(z\right) = \frac{\bar{R}\left(\bar{z}\right)}{\bar{L}}, r = \frac{\bar{r}}{\bar{L}}, t = \bar{t}\,\bar{\omega}_P, \omega = \frac{\bar{\omega}_0}{\bar{\omega}_P}, d_s = \frac{\bar{d}_s}{\bar{L}}, u = \frac{4\,\upsilon\,\rho\,\bar{u}}{P_0\,\bar{L}^2},$$

$$B' = \frac{\rho\, g}{P_0}, V_s = \frac{4\,\upsilon\,\rho\,\bar{V}_s}{P_0\,\bar{L}^2}, \tau = \frac{2\,\bar{\tau}}{P_0\,\bar{L}}, \varepsilon^2 = \frac{\bar{L}^2\,\bar{\omega}_P}{\upsilon}, \varepsilon_0 = \frac{P_1}{P_0}, B = \frac{f_0}{P_0},$$

$$M = \frac{\sigma\,\bar{B}^2\,\bar{L}^2}{\upsilon\,\rho}, K = \frac{\bar{K}}{\bar{L}^2}, d_0 = \frac{\bar{d}_0}{\bar{L}}, \mu_E = \frac{\bar{\mu}_E}{8\,\upsilon\,\rho}, d = \frac{\bar{d}}{\bar{L}} \tag{8}$$

Where ε, M, K and d_s are respectively the Pulsatile Reynolds number or the Womersley frequency parameter, Hartmann number or magnetic parameter, the permeability parameter and the dimensionless height of the stenosis. The remaining quantities relevant to this problem are described at their appropriate places. We substitute the quantities defined in (8) into (1), (2), (4), (5), (6) and (7) and then simplifying, we get the following in non-dimensional forms:

Non-dimensional form of the geometry of arterial stenosis is:

$$R\left(z\right) = \begin{cases} 1 - m\left(z+d\right) - \dfrac{d_s \cos\phi}{2}\left(1 + \cos\dfrac{\pi z}{d_0}\right), & \text{for } \left|z\right| \le d_0 \\ 1 - m\left(z+d\right), & \text{for } \left|z\right| > d_0 \end{cases} \tag{9}$$

Momentum equation:

$$\varepsilon^2 \frac{\partial u}{\partial t} = 4\left\{B\cos\left(\omega t + \theta\right) + B'\cos\beta + \left(1 + \varepsilon_0 \cos t\right)\right\} + \frac{1}{r}\frac{\partial}{\partial r}\left(r\frac{\partial u}{\partial r}\right) - \left(M + \frac{1}{K}\right)u \tag{10}$$

Subject to the following non-dimensional boundary conditions:

$$u = V_s \text{ at } r = R \tag{11}$$

$$\frac{\partial u}{\partial r} = 0 \text{ at } r = 0 \tag{12}$$

Where u is finite at $r = 0$.

3. METHOD OF SOLUTION

Assuming the Pulsatile Reynolds number ε to be very small, the velocity u may be approximated by the following series (perturbation technique):

$$u(z,r,t) = v_0(z,r,t) + \varepsilon^2 v_1(z,r,t) + \ldots\ldots \tag{13}$$

Substituting (13) in (10), (11) and (12) and equating the coefficients of ε^0 and ε^2 and then neglecting the terms containing higher powers of ε, we obtain:

$$0 = 4h(t) + \frac{1}{r}\frac{\partial}{\partial r}\left(r\frac{\partial v_0}{\partial r}\right) - \left(M + \frac{1}{K}\right)v_0 \tag{14}$$

$$\frac{\partial v_0}{\partial t} = \frac{1}{r}\frac{\partial}{\partial r}\left(r\frac{\partial v_1}{\partial r}\right) - \left(M + \frac{1}{K}\right)v_1 \tag{15}$$

Where $h(t) = B\cos(\omega t + \theta) + B'\cos\beta + (1 + \varepsilon_0 \cos t)$.

The corresponding boundary conditions are as under:

$$v_0 = V_s,\ v_1 = 0 \text{ at } r = R \tag{16}$$

$$\frac{\partial v_0}{\partial r} = 0,\ \frac{\partial v_1}{\partial r} = 0 \text{ at } r = 0 \tag{17}$$

The solution of the equations (14), (15) subject to the boundary conditions (16), (17) are as under:

$$v_0 = \left[c_1 J_0\left(r i\sqrt{K_1}\right) + \frac{4}{(K_1)}\right]h(t), \text{ where } c_1 = \frac{\left[\frac{V_s}{h(t)} - \frac{4}{(K_1)}\right]}{J_0\left(R i\sqrt{(K_1)}\right)},$$

$v_1 = V(r)h'(t)$, where $h'(t)$ represents the derivative of $h(t)$ with respect to t;

$$V(r) = c_1 J_0\left(r i\sqrt{K_1}\right)\left[\frac{r^2}{4} + \psi(r) + c_2\right] - \frac{4}{K_1^2},$$

Where, $\psi(r) = \frac{1}{2}\int_0^r x\frac{J_1^2\left(x i\sqrt{(K_1)}\right)}{J_0^2\left(x i\sqrt{(K_1)}\right)}dx = -\frac{1}{2K_1}\left[\frac{r i\sqrt{K_1}\,J_1\left(r i\sqrt{K_1}\right)}{J_0\left(r i\sqrt{K_1}\right)} + \frac{r^2 K_1}{2}\right]$

Where $K_1 = M + \frac{1}{K}$ and $c_2 = \frac{4}{K_1^2 c_1 J_0\left(R i\sqrt{K_1}\right)} - \frac{R^2}{4} - \psi(R)$.

Consequently, the non-dimensional axial velocity $u(z,r,t)$ is given by:

$$u(z,r,t)=v_0(z,r,t)+\varepsilon^2 v_1(z,r,t)$$

3.1. Non-dimensional Wall Shear Stress

Assuming the constricted wall of this artery to be rigid, the non-dimensional wall shear stress τ at $r=R$ is given by:

$$\tau=\frac{2\bar{\tau}}{P_0\bar{L}},$$

Where $\bar{\tau}=-\upsilon\rho\left(\frac{\partial\bar{u}}{\partial\bar{r}}\right)_{\bar{r}=\bar{R}}$ is the dimensional wall shear stress at $\bar{r}=\bar{R}$.

Consequently, we get:

$$\tau=-\frac{1}{2}\left(\frac{\partial u}{\partial r}\right)_{r=R}=-\frac{1}{2}\left[\left(\frac{\partial v_0}{\partial r}\right)_{r=R}+\varepsilon^2\left(\frac{\partial v_1}{\partial r}\right)_{r=R}\right], \text{ where}$$

$$\left(\frac{\partial v_0}{\partial r}\right)_{r=R}=-h(t)c_1 i\sqrt{K_1}\,J_1\left(Ri\sqrt{K_1}\right),$$

$$\left(\frac{\partial v_1}{\partial r}\right)_{r=R}=h'(t)\left[\frac{R}{2}c_1 J_0\left(Ri\sqrt{K_1}\right)\left\{1+\frac{J_1^{\,2}\left(Ri\sqrt{K_1}\right)}{J_0^{\,2}\left(Ri\sqrt{K_1}\right)}\right\}-\frac{4i\sqrt{K_1}\,J_1\left(Ri\sqrt{K_1}\right)}{K_1^{\,2}J_0\left(Ri\sqrt{K_1}\right)}\right].$$

3.2. Non-dimensional Volumetric Flow Rate

The dimensionless volumetric flow rate $Q(z,t)$ may be defined as under:

$Q(z,t)=\frac{8\upsilon\rho\,\bar{Q}(\bar{z},\bar{t})}{\pi\bar{L}^4P_0}$, where $\bar{Q}(\bar{z},\bar{t})$ is the dimensional volumetric flow rate and is given by $\bar{Q}(\bar{z},\bar{t})=2\pi\int_0^{\bar{R}}\bar{r}\,\bar{u}(\bar{z},\bar{r},\bar{t})\,d\bar{r}$.

Consequently, $Q(z,t)=4\int_0^R r\,u(z,r,t)\,dr=I_0+I_1$, where,

$$I_0=4\int_0^R r\,v_0(z,r,t)\,dr=\frac{4h(t)}{K_1}\left[2R^2-c_1 Ri\sqrt{K_1}\,J_1\left(Ri\sqrt{K_1}\right)\right],$$

$$I_1 = 4\varepsilon^2 \int_0^R r\, v_1(z, r, t)\, dr$$

$$= \frac{4\varepsilon^2 h'(t)}{K_1}\left[\left\{ -\frac{c_1 R^3 i\sqrt{K_1}}{4} - c_1 R i\sqrt{K_1}\,\psi(R) \right.\right.$$

$$\left.\left. - c_1 c_2 R i\sqrt{K_1}\right\} J_1\left(R i\sqrt{K_1}\right) + \frac{c_1 R^2}{2} J_2\left(R i\sqrt{K_1}\right) \right.$$

$$\left. - \frac{2R^2}{K_1} + \frac{c_1 i\sqrt{K_1}}{2}\int_0^R \frac{r^2 J_1^3\left(r i\sqrt{K_1}\right)}{J_0^2\left(r i\sqrt{K_1}\right)} dr \right],$$

where $\int_0^R \frac{r^2 J_1^3\left(r i\sqrt{K_1}\right)}{J_0^2\left(r i\sqrt{K_1}\right)} dr = \frac{i}{K_1\sqrt{K_1}}\left[\frac{-R^2 K_1 J_1^2\left(R i\sqrt{K_1}\right)}{J_0\left(R i\sqrt{K_1}\right)} + 2R^2 K_1 J_2\left(R i\sqrt{K_1}\right)\right].$

3.3. Non-dimensional Effective Viscosity

Following Pennington and Cowin [28], the effective viscosity $\overline{\mu}_E$ in dimensional form may be expressed as follows:

$$\overline{\mu}_E = \frac{\pi\left(-\frac{\partial \overline{P}\left(\bar{z},\bar{t}\right)}{\partial \bar{z}}\right)\left(\overline{R}\left(\bar{z}\right)\right)^4}{\overline{Q}\left(\bar{z},\bar{t}\right)}$$

$$\Rightarrow \mu_E = \frac{\left(1+\varepsilon_0\cos t\right)R^4}{Q(z,t)}$$

Where μ_E is the non-dimensional effective viscosity.

4. RESULTS AND DISCUSSION

In order to get an insight into the biological and physical aspects of this problem, we obtain the profiles of the axial velocity, wall shear stress, volumetric flow rate and the effective viscosity, and we examine their behaviors under the influence of the various non-dimensional parameters relevant to this problem. The data-tabulation involved in this problem is carried out with the aid of Python(x, y) v2.7.6.10, using the packages: cmath, mpmath and numpy. For all the figures, we take $\omega = \frac{\pi}{9}, \theta = \frac{\pi}{4}, z = 0.2, d = 0.5, \varepsilon = 0.2,\ d_0 = 0.34, \varepsilon_0 = 0.5,$ and $d_s = 0.24$. For

calculations on axial speed *u*, we take $\phi = \frac{\pi}{90}$. Clearly, $r \in [0, R]$ and using (9) and then noting that $|z| < d_0$ for the aforementioned choice of z, d_0, we find that $R = 0.888448116$. Thus, for our choice of z, d_0 and ϕ, we get $r \in [0, 0.888448116]$. For the remaining calculations, the values of the parameters have been specified along with the relevant figures.

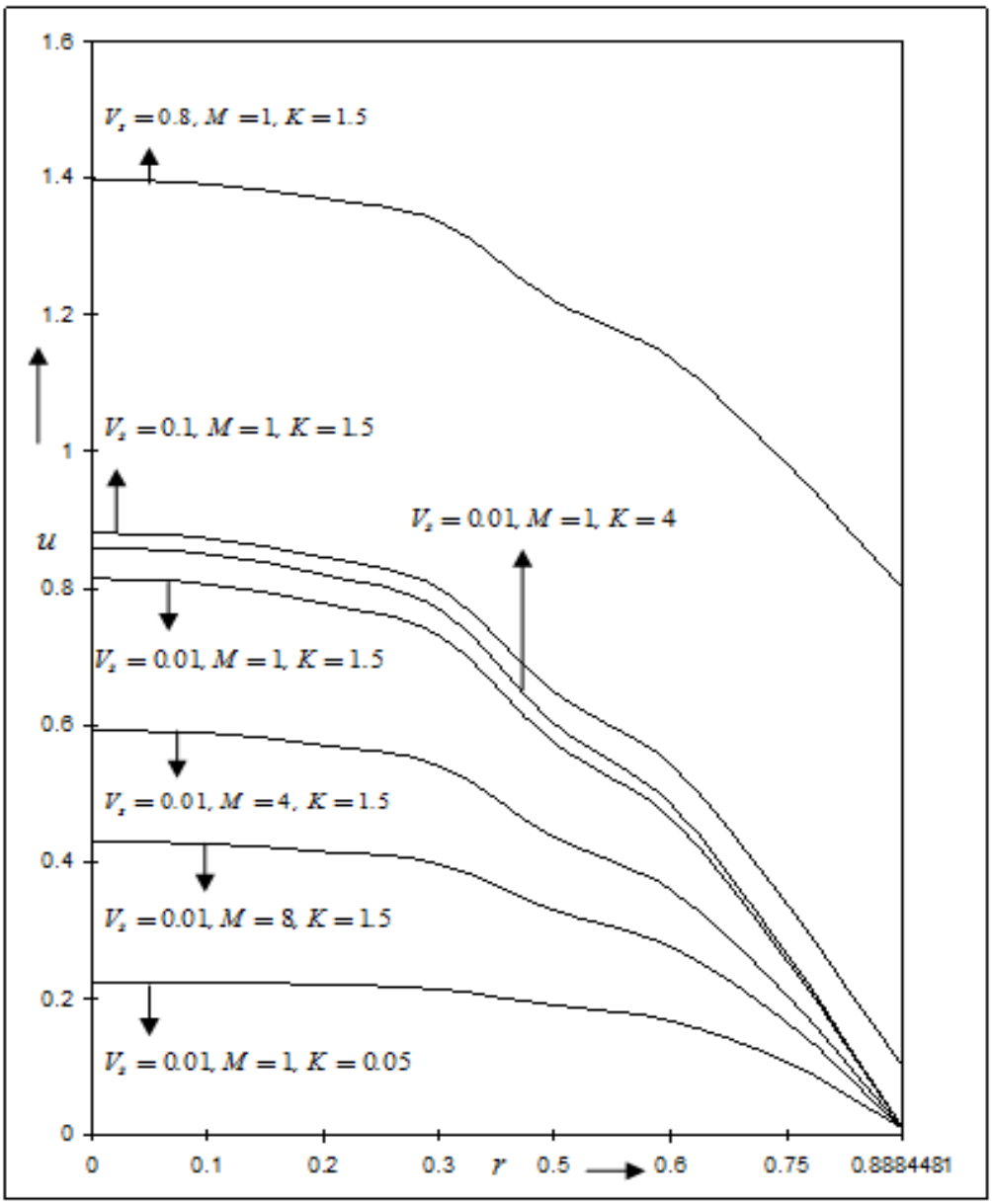

Figure 1: Axial speed *u* versus *r*, under *M*, *K* and V_s,

for $t = 1$, $\beta = \frac{\pi}{2}$, $B = 0.02$, $B' = 0$, $\phi = \frac{\pi}{90}$.

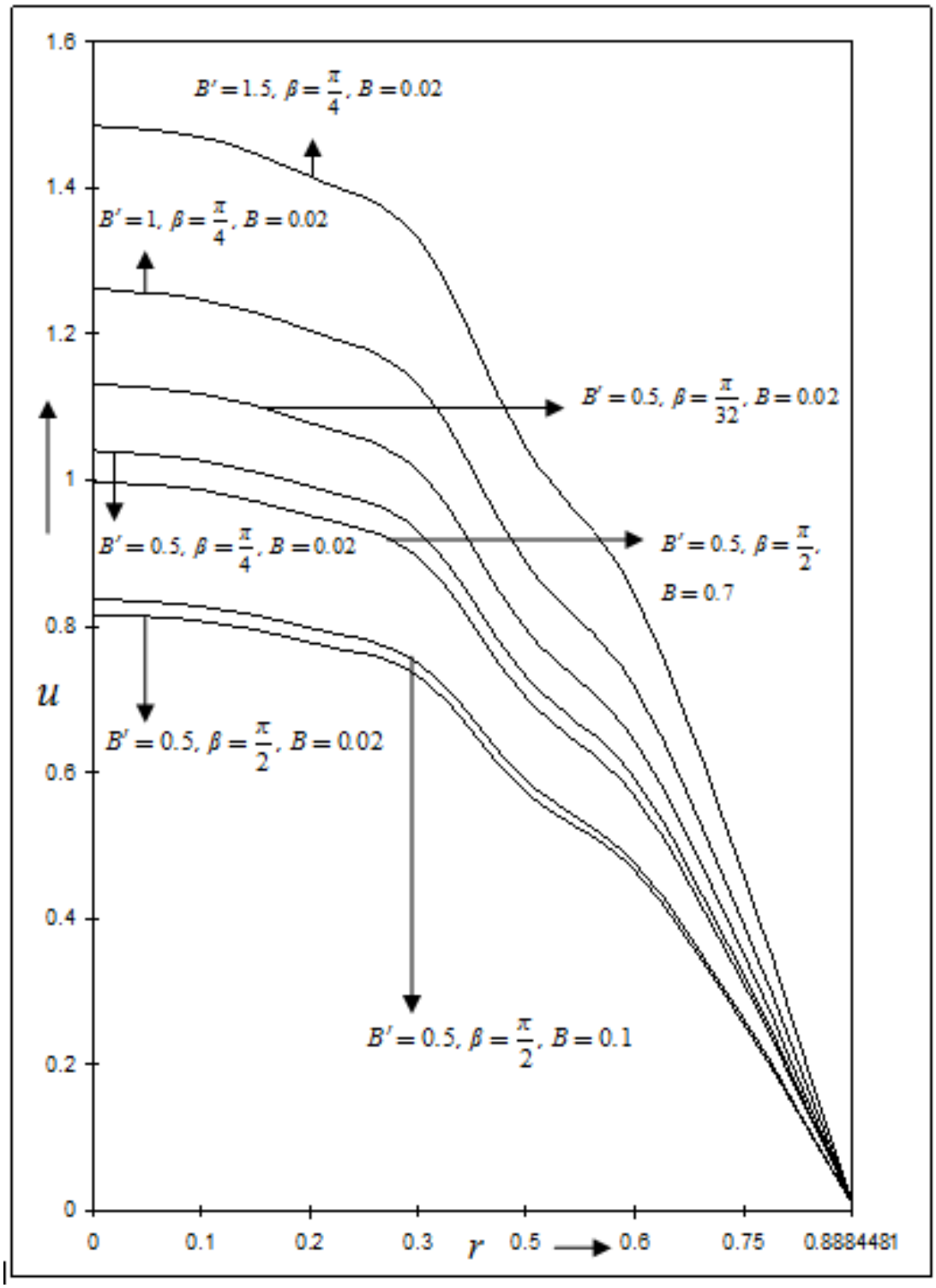

Figure 2: Axial speed u versus r, under B, B' and β,

for $t = 1,\ M = 1, K = 1.5,\ V_s = 0.01,\ \phi = \frac{\pi}{90}$.

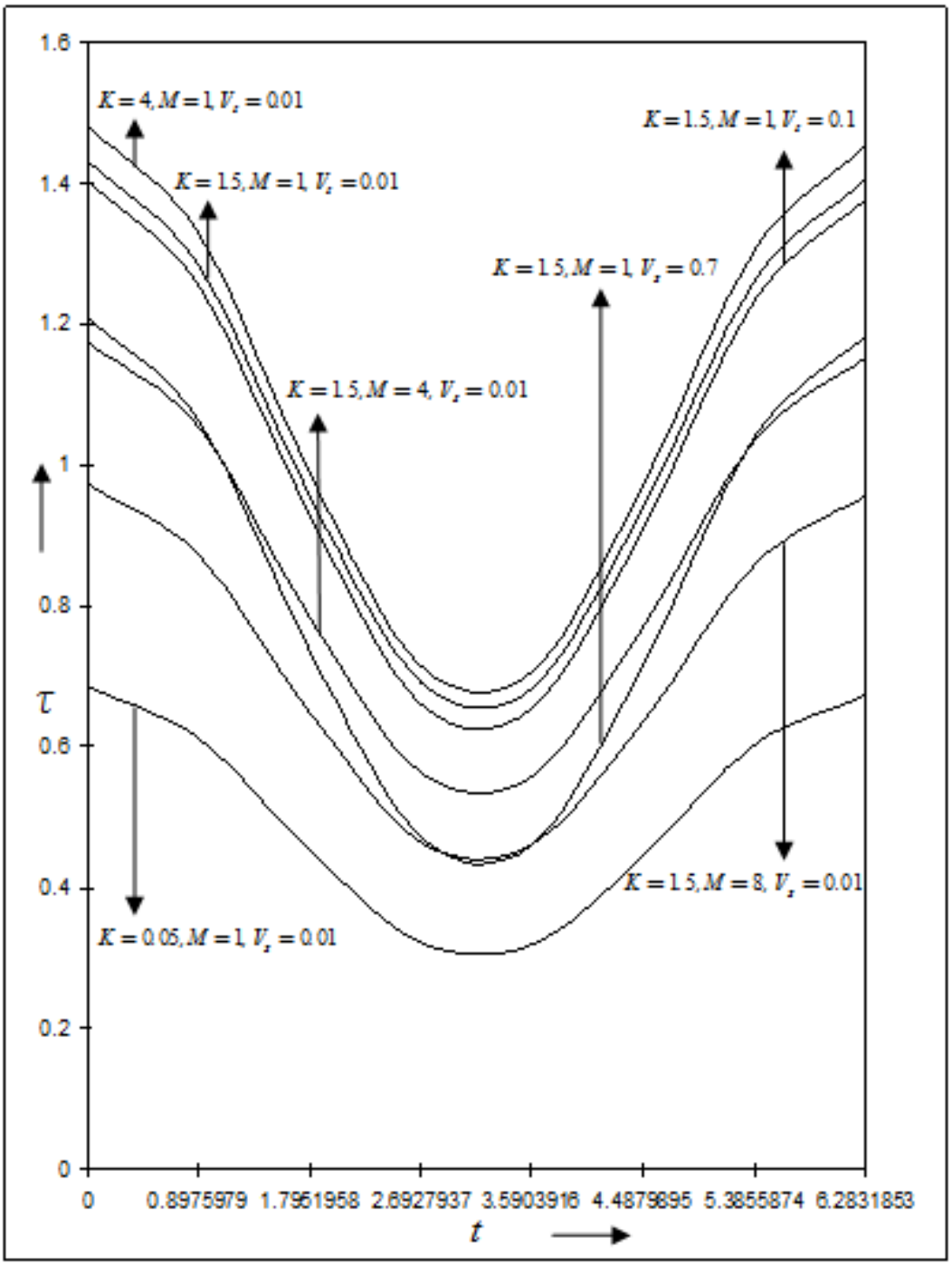

Figure 3: Shear stress τ versus t, under M, K and V_s, for $\beta = \frac{\pi}{4}$, $B = 0.02$, $B' = 0.5$, $\phi = \frac{\pi}{90}$.

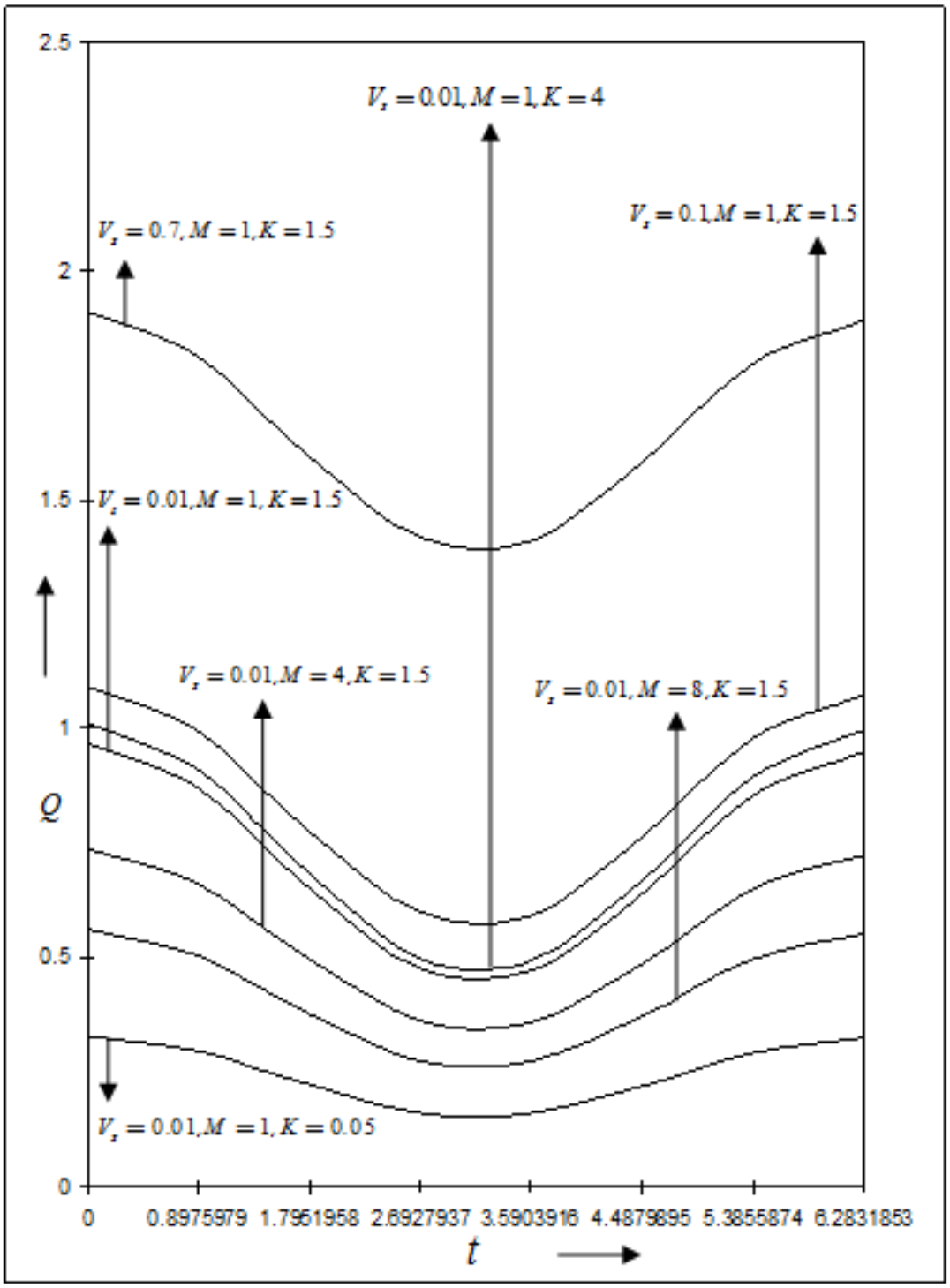

Figure 4: Volumetric flow rate Q versus t, under M, K and V_s, for $\beta = \frac{\pi}{4}$, $B = 0.02$, $B' = 0.5$, $\phi = \frac{\pi}{90}$.

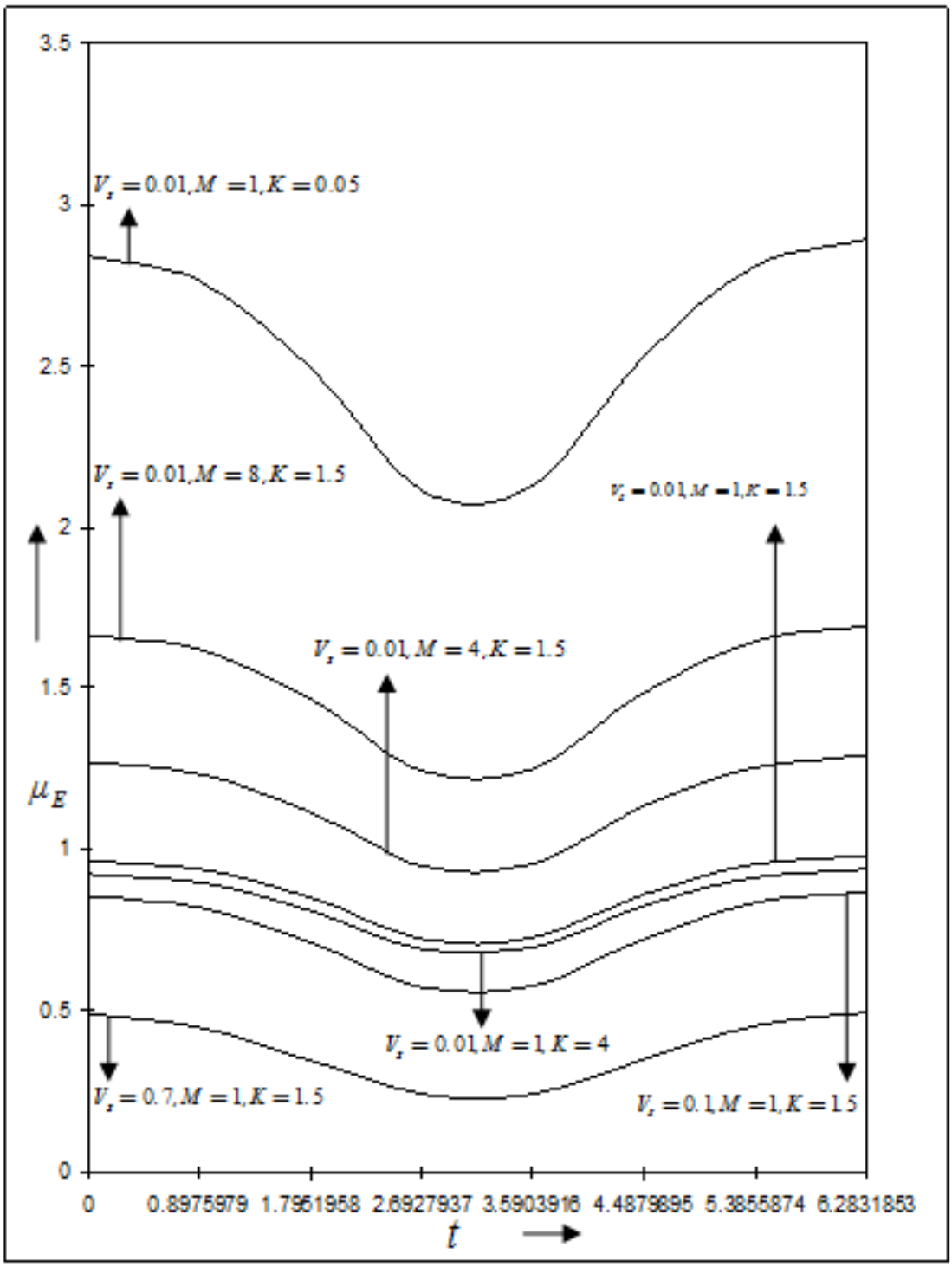

Figure 5: Effective viscosity μ_E versus t, under M, K and V_s, for $\beta = \frac{\pi}{4}$, $B = 0.02$, $B' = 0.5$, $\phi = \frac{\pi}{90}$.

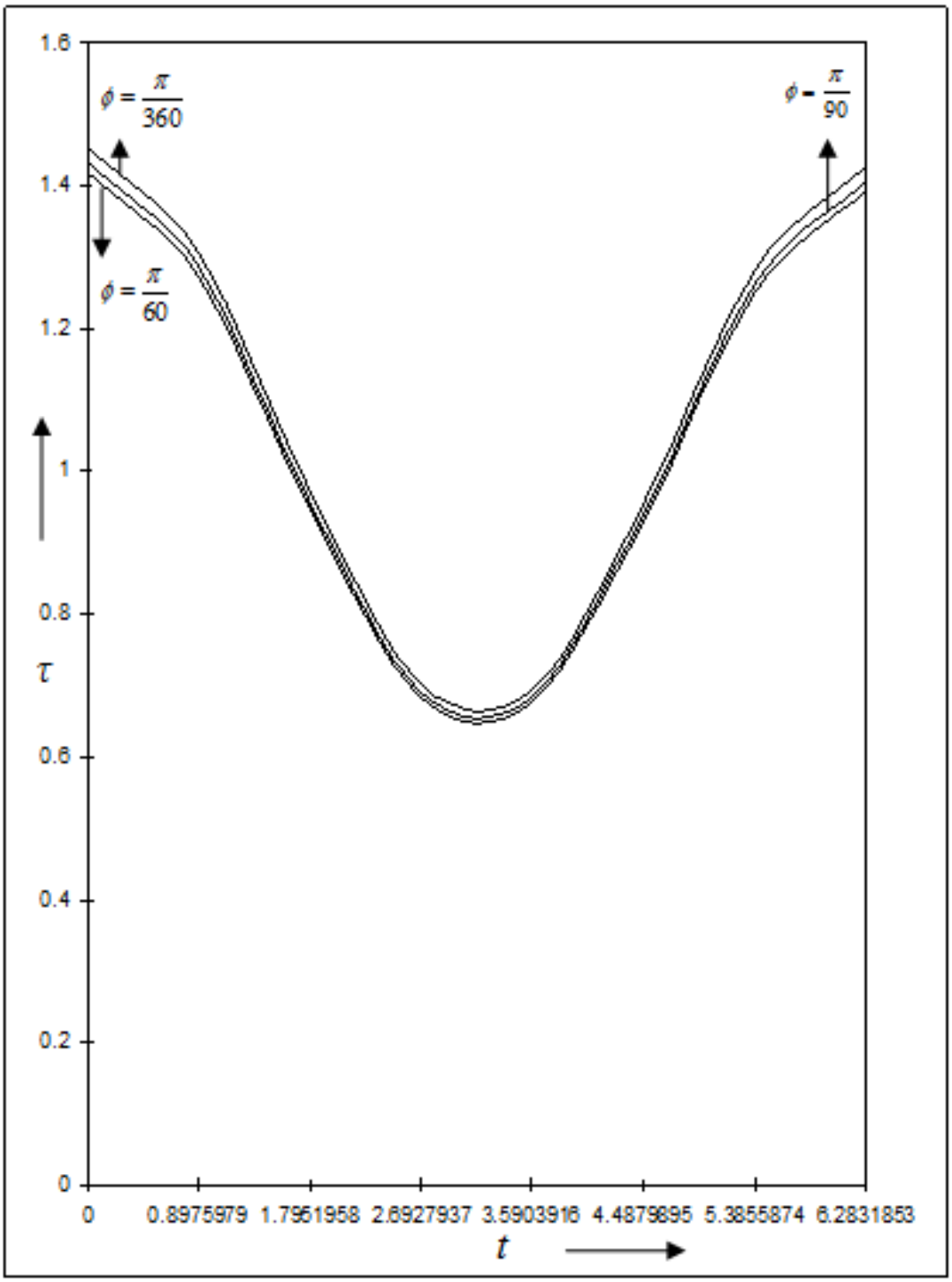

Figure 6: Shear stress τ versus t, under ϕ,

for $\beta = \frac{\pi}{4}$, $B = 0.02$, $B' = 0.5$, $K = 1.5$, $M = 1$, $V_s = 0.01$

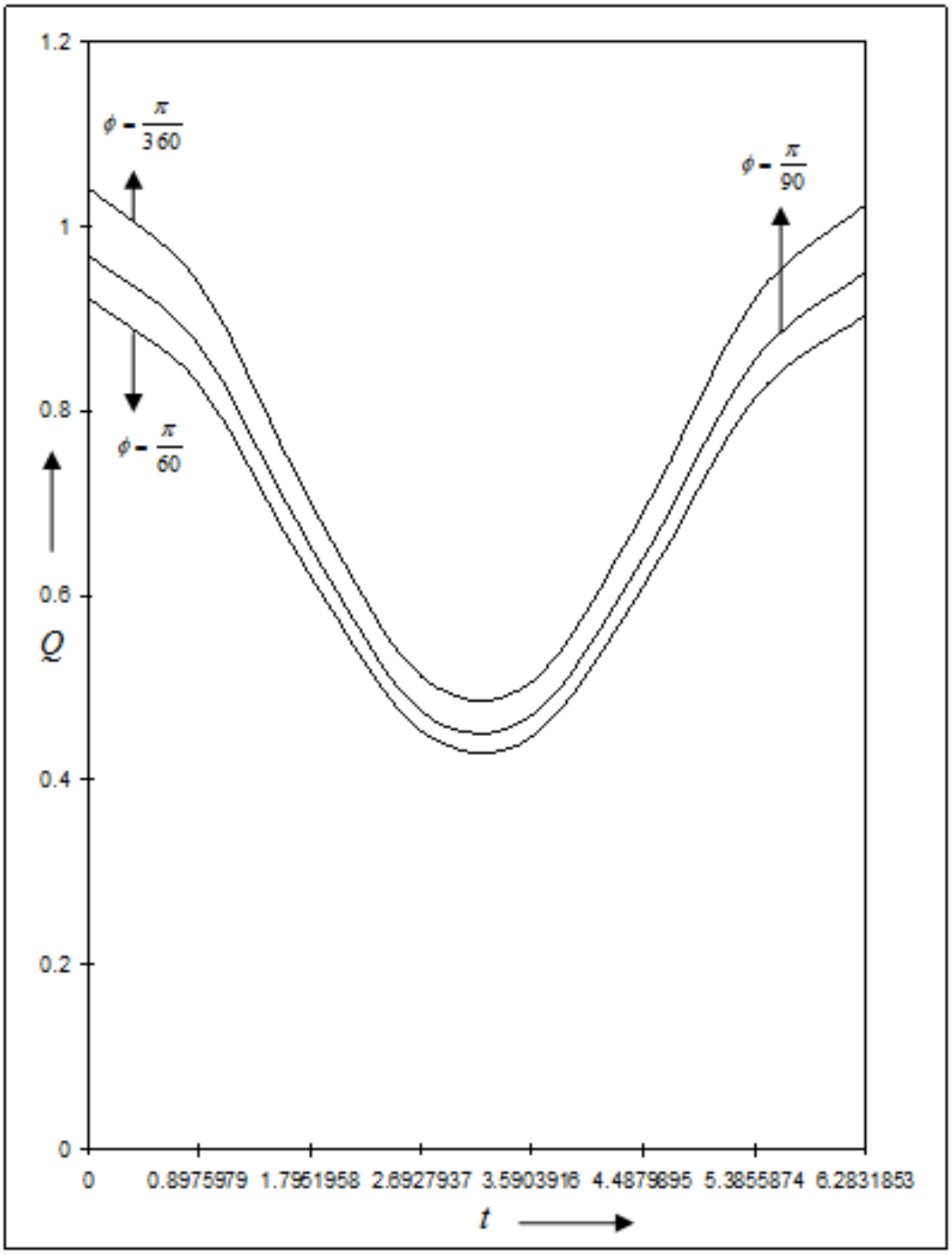

Figure 7: Volumetric flow rate Q versus t, under ϕ,

for $\beta = \frac{\pi}{4}$, $B = 0.02$, $B' = 0.5$, $K = 1.5$, $M = 1$, $V_s = 0.01$

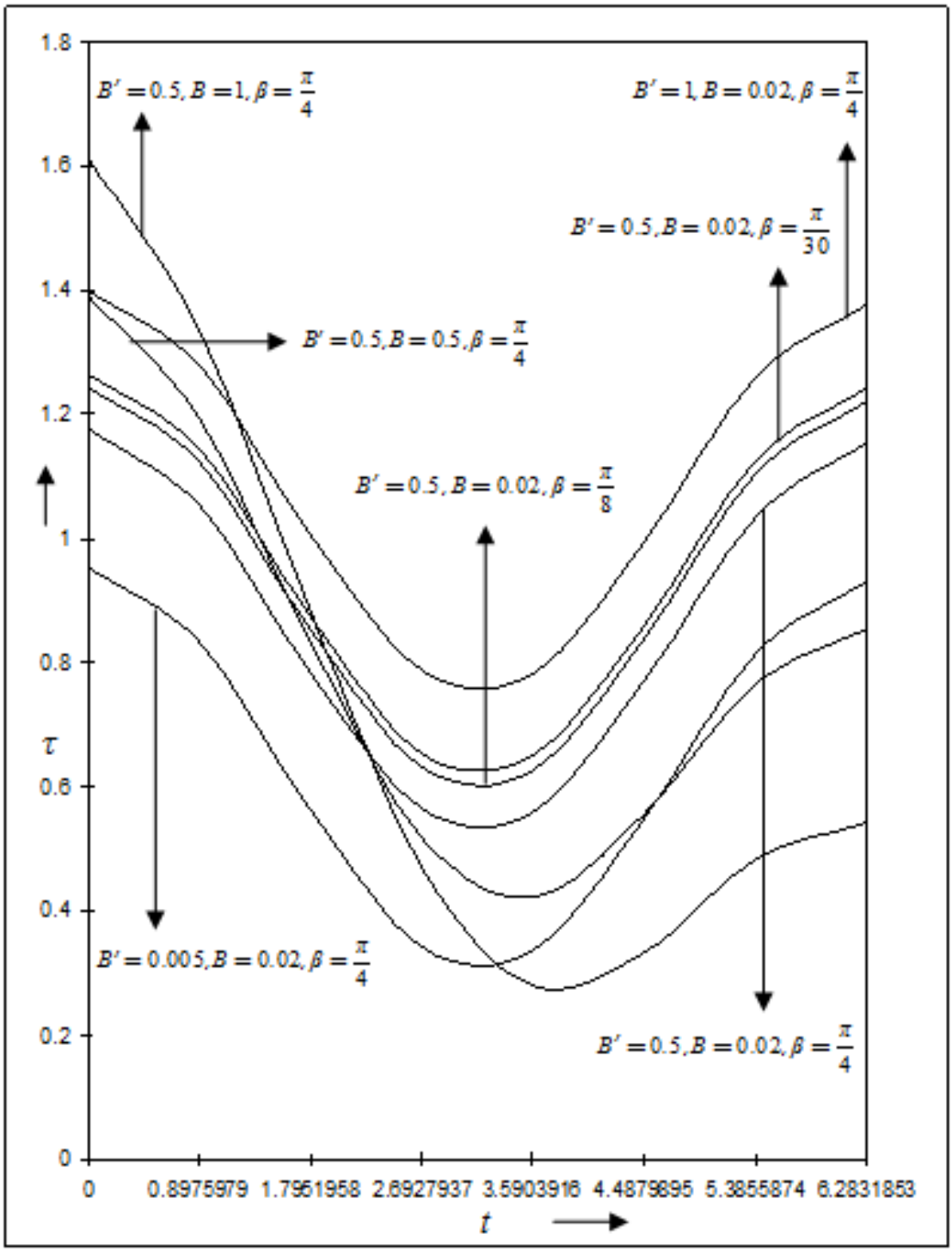

Figure 8: Shear stress τ versus t, under β, B, B',

for $K = 1.5$, $M = 4$, $V_s = 0.01$, $\phi = \frac{\pi}{90}$

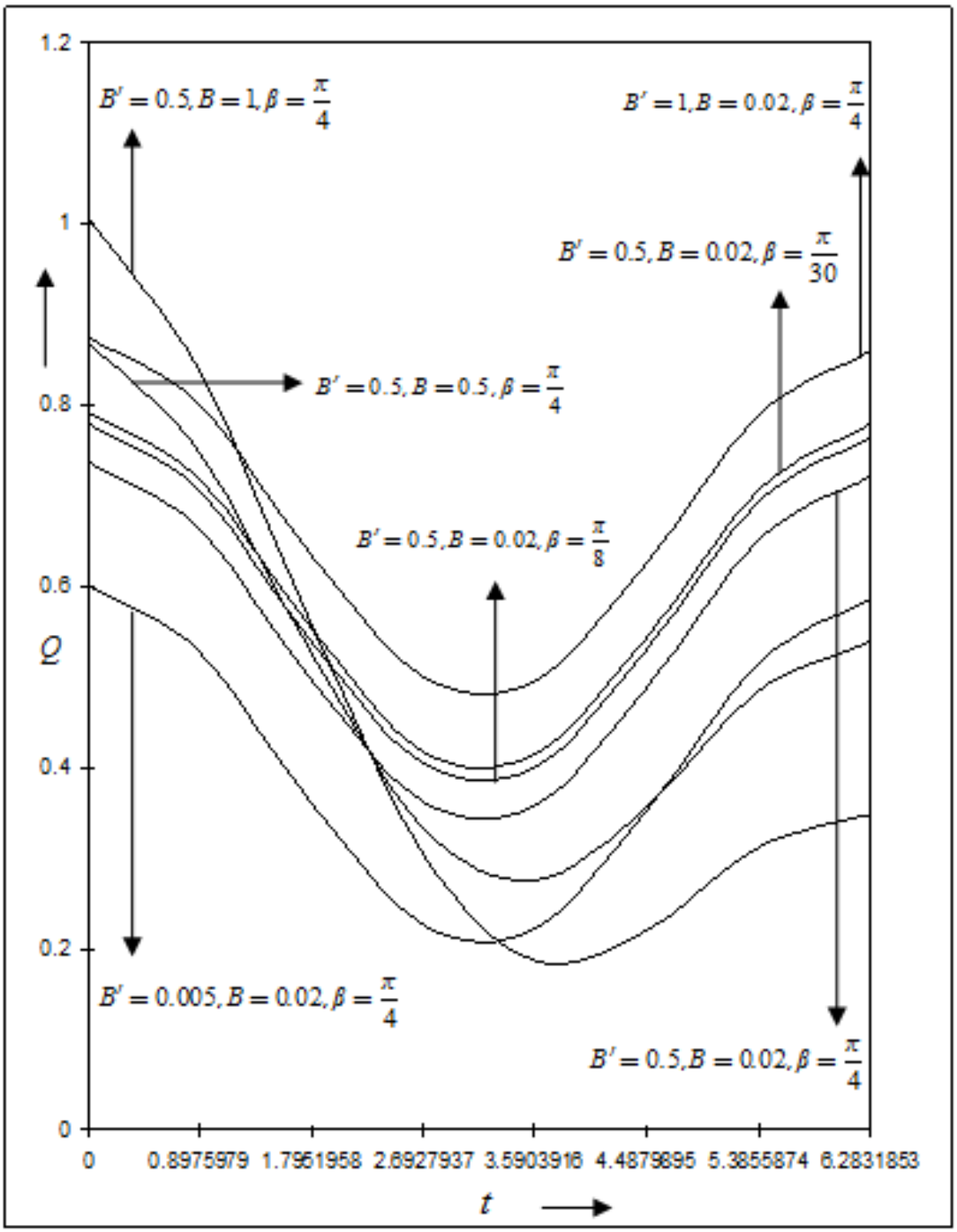

Figure 9: Volumetric flow rate Q versus *t*, under β, B, B',

for $K = 1.5$, $M = 4$, $V_s = 0.01$, $\phi = \frac{\pi}{90}$

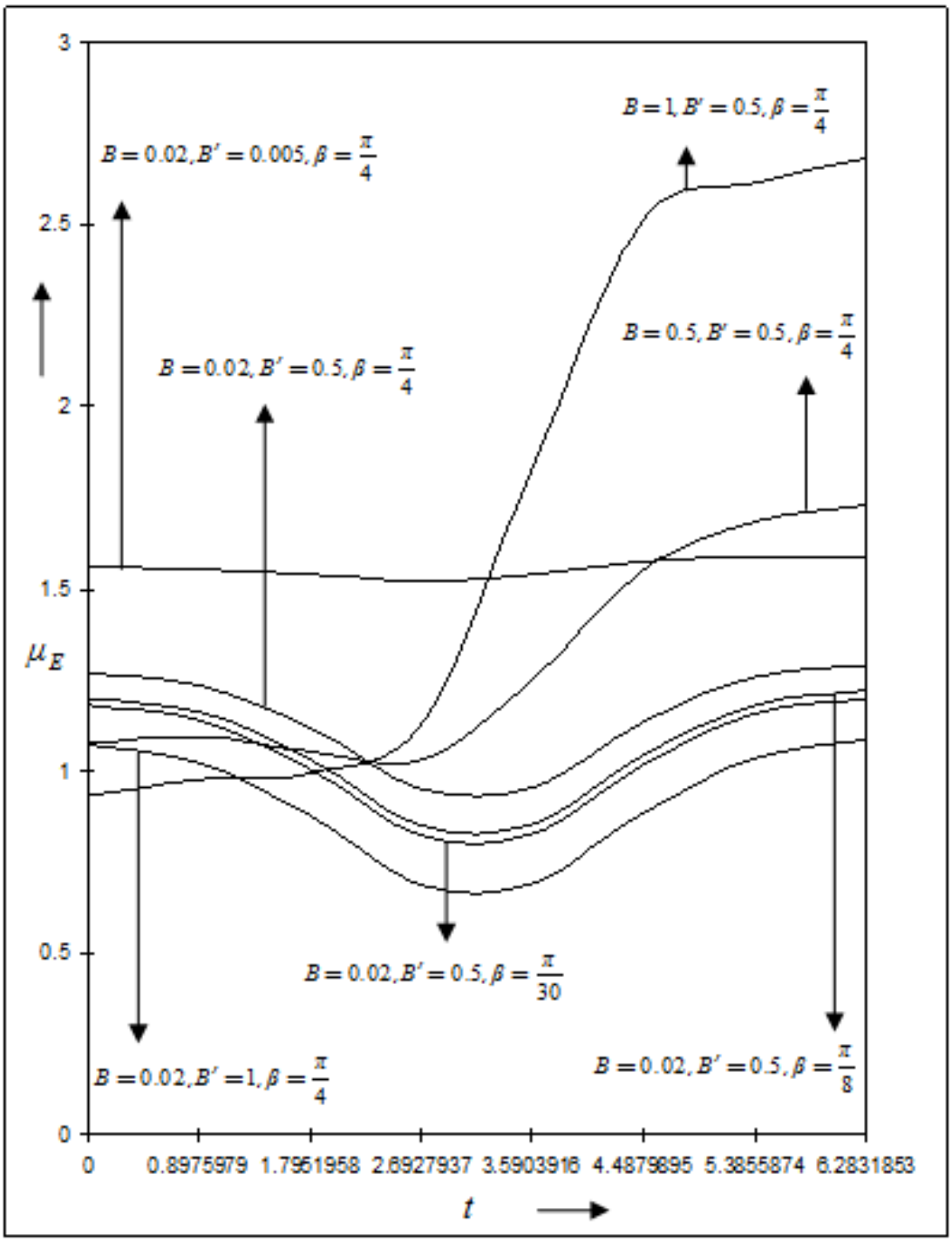

Figure 10: Effective viscosity μ_E versus *t*, under β, B, B',

for $K = 1.5$, $M = 4$, $V_s = 0.01$, $\phi = \frac{\pi}{90}$

Table 1: Effective viscosity μ_E versus t, under ϕ,

for $\beta = \frac{\pi}{4}$, $B = 0.02$, $B' = 0.5$, $K = 1.5$, $M = 1$, $V_s = 0.01$

t	$\mu_E\ (\phi = \frac{\pi}{360})$	$\mu_E\ (\phi = \frac{\pi}{90})$	$\mu_E\ (\phi = \frac{\pi}{60})$
0	0.971921595	0.96427674425	0.95925202426
$\frac{2\pi}{7}$	0.945609325	0.93814573648	0.93323813217
$\frac{4\pi}{7}$	0.856268732	0.84935890191	0.84480966141
$\frac{6\pi}{7}$	0.727501906	0.72140156741	0.71737849214
$\frac{8\pi}{7}$	0.733754132	0.72754597371	0.72345192321
$\frac{10\pi}{7}$	0.871054945	0.86391903109	0.85922105090
$\frac{12\pi}{7}$	0.962789093	0.95511641619	0.95007122576
2π	0.989637344	0.98184329564	0.97672018945

The flow configuration for arterial stenosis

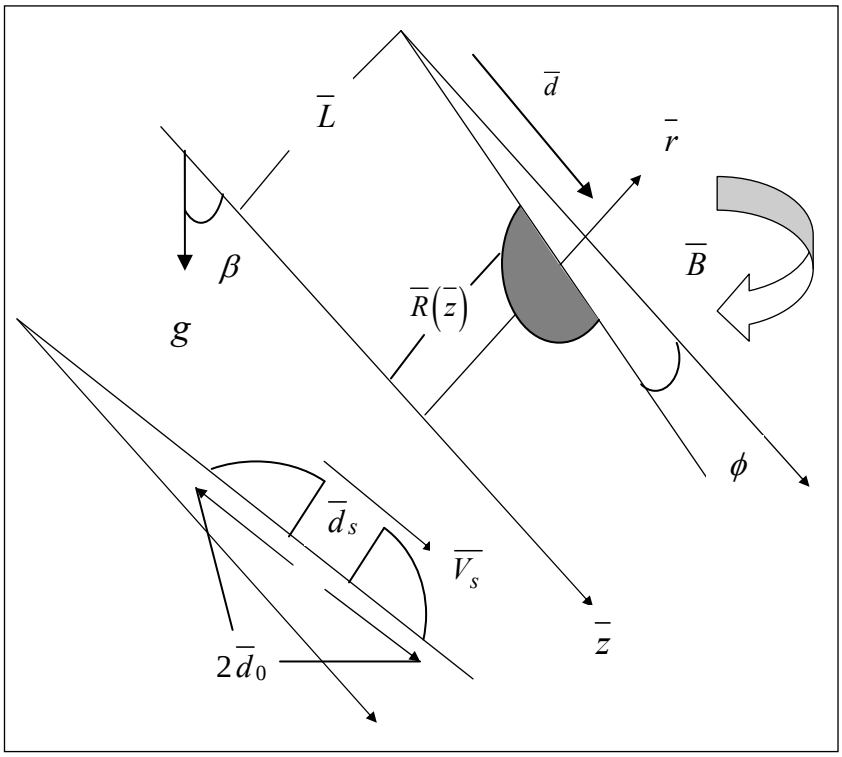

From **Figure 1**, we observe that the axial speed u decreases as the magnetic field strength increases, while the axial speed rises with a growth in each of slip velocity and porosity of the medium. **Figure 2** depicts that an increase in the angle of inclination (β) leads to a fall in the axial speed u whereas the axial speed rises with a rise in each of B, B'. It may be emphasized that B represents the relative effectiveness of the amplitude of body acceleration (f_0) over the steady state pressure gradient (P_0). Further, B' signifies the relative efficacy of the gravitational body force (ρg) over the steady state pressure gradient (P_0). From both these figures, it is noted that the axial speed decreases with an increase in the radial distance from the axis towards the stenosed wall. Thus, the maximum speed occurs at the axis of the artery.

Figures 3 and **6** show that the wall shear stress τ registers a growth with a growth in the porosity of the medium, whereas a growth in each of magnetic field strength, slip velocity and tapering angle causes the wall shear stress to decrease.

Also, the **Figures 4** and **7** indicate that the volumetric flow rate Q registers a decline with a rise in each of the strength of the magnetic field and the tapering angle, while the volumetric flow rate increases when each of porosity, and slip velocity increases.

Further, the **Figure 5** and **Table 1** show that the Effective viscosity μ_E decreases when each of slip velocity, porosity and tapering angle increase whereas the Effective viscosity registers a growth when the magnetic field strength rises.

Figure 8 shows that the shear stress falls as the angle of inclination increases whereas an increase in B' leads to a rise in shear stress. However, the shear stress first increases and then again decreases as B increases. This is attributable to the pulsatile pressure gradient and the periodic body acceleration (as evident from the definition of B).

Figure 9 indicates that the volumetric flow rate decreases as the angle of inclination increases while an increase in B' causes a growth in the volumetric flow rate. However, a growth in B causes Q to first increase and then again decrease. This is due to the pulsatile pressure gradient and the periodic body acceleration (as apparent from the definition of B).

Figure 10 indicates that the effective viscosity rises with a rise in the angle of inclination whereas the effective viscosity falls as B' increases. But the effective viscosity first decreases and then again increases as B increases. This is because of the pulsatile pressure gradient and the periodic body acceleration (as seen from the definition of B).

It may also be observed from the **Figures 3**, **4**, **5**, **6**, **7, 8, 9,** and **10** and **Table 1** that each of Wall shear stress, Volumetric flow rate and Effective viscosity first decreases and then again increases as the dimensionless time t increases from 0 to 2π i.e. for one full cycle (complete period) of body acceleration. The wavy nature of the profiles

as evident from the **Figures 3**, **4**, **5**, **6**, **7, 8, 9,** and **10** and **Table 1** may be attributed to the effects of the pulsatile pressure gradient (that contains the periodic function $\cos\left(\overline{\omega}_P \bar{t}\right)$) and the periodic body acceleration $\overline{F}\left(\bar{t}\right)$.

5. CONCLUSIONS:

We arrive at the following conclusions, based on our results:

1. The imposition of the magnetic field causes a decrease in axial speed of blood. Thus the azimuthal magnetic field is helpful in controlling the axial blood flow speed.
2. The growth in porosity as well as the velocity slip leads to a corresponding growth in the blood flow speed. This suggests that the blood flow through such stenosed arteries may be enhanced by increasing porosity as well as by the possible development and application of slip inducing drugs.
3. An increase in the angle of inclination (to the vertical) leads to a fall in the axial speed.
4. When the body acceleration increases, the blood flow speed also rises i.e. the heart has to pump blood at a faster rate whenever the patient performs some strenuous action. Hence, patients with cardio-vascular diseases should avoid strenuous action in order to avoid undue stress on the heart.
5. Rise in gravitational body force causes the blood flow speed to increase.
6. The maximum blood flow speed occurs on the axis of the artery.
7. The wall shear stress exhibits a growth in magnitude with an increase in the porosity of the medium.
8. A growth in each of magnetic field strength, angle of inclination, slip velocity and tapering angle causes the wall shear stress to decline. Evidently, this raises the prospects for minimizing shear stress at the arterial walls by using azimuthal magnetic field together with the possible development and application of velocity slip inducing drugs. An increase in the tapering of inner arterial walls will lead to a decline in the arterial wall shear stress. It is also seen that the wall shear stress increases when the relative efficacy of the gravitational body force over the steady state pressure gradient increases. Consequently, the wall shear stress (blood pressure) rises as the density of blood increases. It is further observed that the wall shear stress first rises and then falls as the relative effectiveness of the amplitude of body acceleration over the steady state pressure gradient increases. This is due to the pulsatile pressure gradient and the periodic body acceleration. To avoid drastic fluctuations in blood pressure, patients with cardio-vascular diseases should avoid activities involving excessive body accelerations.

9. The volumetric flow rate exhibits a fall with a growth in each of magnetic field strength, angle of inclination and the angle of tapering, whereas the volumetric flow rate enhances with an augmentation in each of porosity and slip velocity. Further, the volumetric flow rate registers a growth with a growth in the relative efficacy of the gravitational body force over the steady state pressure gradient. Evidently, the application of a suitable magnetic field can control the volumetric flow within the stenosed section of the arterial wall. There is also an implication of the possible development of suitable medical procedures to augment porosity and the production and application of slip inducing drugs that will aid in enhancing the volumetric flow rate of blood through stenosed arteries. Furthermore, the volumetric flow rate first increases and then again decreases as the relative effectiveness of the amplitude of body acceleration over the steady state pressure gradient rises. This is due to the pulsatile pressure gradient and the periodic body acceleration.
10. The Effective viscosity falls when each of slip velocity, porosity and tapering angle rises whereas the Effective viscosity records an augmentation when the strength of the magnetic field and the angle of inclination increase. The effective viscosity falls when the relative efficacy of the gravitational body force over the steady state pressure gradient increases. On the other hand, the effective viscosity first decreases and then again increases as the relative effectiveness of the amplitude of body acceleration over the steady state pressure gradient increases. This is because of the pulsatile pressure gradient and the periodic body acceleration.

ACKNOWLEDGEMENT

The authors are highly thankful to CSIR-HRDG for funding this research work under Research Grant-in-aid No. 25(0209)/12/EMR-II.

APPENDIX:

The continuity equation is given by:

$$\frac{\partial q_r}{\partial r}+\frac{1}{r}q_r+\frac{1}{r}\frac{\partial q_\theta}{\partial \theta}+\frac{\partial q_z}{\partial z}=0,$$

Where $\vec{q}=(q_r,q_\theta,q_z)$ is the fluid velocity in cylindrical system of coordinates (r,θ,z).

The direction of the main flow is in the *z*-direction i.e. along the axis of the artery; the artery being assumed to be cylindrical (tubular) in shape. Thus $q_r=0,\ q_\theta=0$ i.e. the radial and tangential velocity components are each zero. Moreover, the flow is axi-symmetric and so q_z is free of θ. Then the above continuity equation yields:

$\frac{\partial q_z}{\partial z}=0 \Rightarrow q_z$ is free of *z*. Also, we recall that q_z is free of θ. Hence, for this transient (time-dependent) flow, q_z depends on only *r*, *t*. Denoting q_z by *u*, we see that the axial speed *u* depends on only *r* and *t*.

REFERENCES

[1] Y. C. Fung, *Biodynamics Circulation*, Springer-Verlag, New York, 1984.

[2] D. A. McDonald, *Blood Flow in Arteries*, Arnold, London, 1960.

[3] M. Zamir, *The Physics of Coronary Blood Flow*, Springer, New York, 2005.

[4] M. W. David, P. M. Christos, R. H. Stephen and N. Ku. David, "A mechanistic model of acute platelet accumulation in thrombogenic stenoses", *Annals of Biomedical Engineering*, vol. **29** (4), (2001), 321-329.

[5] D. F. Young, "Fluid Mechanics of Arterial Stenoses", *Journal of Biomechanical Engineering*, vol. **101**, (1979), 157-175.

[6] Z. R. Liu, G. Xu, Y. Chen, Z. Z. Teng and K. R. Qin, "An Analysis Model of Pulsatile Blood Flow in Arteries", *Applied Mathematics and Mechanics*, vol. **24**, (2003), 230-240.

[7] L. Yao and D. Z. Li, "Pressure and Pressure Gradient in an Axisymmetric Rigid Vessel with Stenosis", *Applied Mathematics and Mechanics*, vol. **27**, (2006), 347-351.

[8] Kh. S. Mekheimer and M. A. El Kot, "Influence of Magnetic Field and Hall Currents on Blood Flow through a Stenotic Artery", *Applied Mathematics and Mechanics*, vol. **29**, (2008), 1093-1104.

[9] V. K. Sud and G. S. Sekhon, "Blood flow subject to a single cycle of body acceleration", *Bulletin of Mathematical Biology*, vol. **46**, (1984), 937-949.

[10] M. El-Shahed, "Pulsatile flow of blood through a stenosed porous medium under periodic body acceleration", *Appl. Math. Comput.*, vol. **138**, (2003), 479-488.

[11] E. F. Elshehawey, E. M. E. Elbarbary, M. E. Elsayed, N. A. S. Afifi and M. El-Shahed, "Pulsatile flow of blood through a porous medium under periodic body acceleration", *Int. J. Theoretical Phys*., vol. **39 (**1), (2000), 183-188.

[12] P. Brunn, "The Velocity Slip of Polar Fluids", *Rheol. Acta*., vol. **14**, (1975), 1039-1054.

[13] A. L. Jones, "On the Flow of Blood in a Tube", *Biorheology*, vol. **3**, (1966), 183-188.

[14] L. Bennet, "Red Cell Slip at a Wall", *in vitro*. *Science*, vol. **155**, (1967), 1554-1556.

[15] G. Bugliarello and J. W. Hayden, "High Speed Micro Cinematographic Studies of Blood Flow", *in vitro*. *Science*, vol. **138**, (1962), 981-983.

[16] G. Astarita and G. Marrucci, *Principles of Non-Newtonian Fluid Mechanics*, McGraw-Hill, New York, USA, 1974.

[17] D. C. H. Cheng, "The Determination of Wall Slip Velocity in the Laminar Gravity Flow of Non-Newtonian Fluids along Plane Surfaces", *Ind. Eng. Chem. Fundamen*., vol. **13**, (1974), 394-395.

[18] A. Kolin, "An Electromagnetic Flowmeter: Principle of Method and Its Application to Blood Flow Acceleration", *Experimental Biology and Medicine*, vol. **35**, (1936), 53-56.

[19] E. M. Korchevskii and L. S. Marochnik, "Magneto Hydrodynamic Version of Movement of Blood", *Biophysics*, vol. **10**, (1965), 411-413.

[20] M. F. Barnothy, *Biological Effects of Magnetic Fields*, Plenum Press, New York, 1964.

[21] Z. L. Xu, JMu, J. Liu, M. M. Kamocka, X. Liu, D. Z. Chen, E. D. Rosen and M. S. Alber, "Multiscale model of venous thrombus formation with surface-mediated control of blood coagulation cascade", *Biophysical Journal*, vol. **98**, (2010), 1723-1732.

[22] Z. L. Xu, N. Chen, M. M. Kamocka, E. D. Rosen and M. S. Alber, "Multiscale Model of Thrombus Development", *Journal of the Royal Society Interface*, vol. **4** (24), (2008), 705-723.

[23] Z. L. Xu, N. Chen, S. Shadden, J. E. Marsden, M. M. Kamocka, E. D. Rosen and M. S. Alber, "Study of blood flow impact on growth of thrombi using a multiscale model", *Soft Matter*, vol. **5**, (2009), 769-779.

[24] J. T. Ottesen, M. S. Olufsen and J. K. Larsen, "Applied Mathematical Models in Human Physiology", *SIAM monographs on mathematical modeling and computation*, (2004).

[25] P. Nagarani and G. Sarojamma, "Effect of body acceleration on pulsatile flow of Casson fluid through a mild stenosed artery", *Korea-Australia Rheology Journal*, vol. **20**, (2008), 189-196.

[26] E. F. EL Shehawey and W. E. L. Sebaei, "Peristaltic transport in a cylindrical tube through a porous medium", *International Journal of Mathematics and Mathematical Sciences*, vol. **24**, (2000), 217-230.

[27] E.E. Tzirtzilakis, "A Mathematical Model for Blood Flow in Magnetic Field", *Physics of Fluids*, vol. **17**, (2005), 1-15.

[28] C. J. Pennington and S. C. Cowin, "The Effective Viscosity of Polar Fluids", *Trans. Soc. Rheol*., vol.**14**, (1970), 219-238.

[29] Guo-Tao Liu, Xian-Ju Wang, Bao-Quan Ai, and Liang-Gang Liu, "Numerical Study of Pulsating Flow Through a Tapered Artery with Stenosis", *Chinese Journal of Physics*, vol. **42**, no. 4-I, (2004), 401-409.